MEASUREMENT OF $\sin^2\theta_W$ AND ρ IN DEEP INELASTIC NEUTRINO–NUCLEON SCATTERING

P.G. REUTENS, F.S. MERRITT

Enrico Fermi Institute and Department of Physics, University of Chicago, Chicago, IL 60637, USA

D.B. MACFARLANE [1], R.L. MESSNER [2], D.B. NOVIKOFF [3], M.V. PUROHIT [4]

California Institute of Technology, Pasadena, CA 91125, USA

R.E. BLAIR, F.J. SCIULLI, M.H. SHAEVITZ

Columbia University, New York, NY 10027, USA

H.E. FISK, Y. FUKUSHIMA [5], B.N. JIN [6], T. KONDO [5], P.A. RAPIDIS, D.D. YOVANOVITCH

Fermi National Accelerator Laboratory, Batavia, IL 60510, USA

A. BODEK, R.N. COLEMAN [4], W.L. MARSH [4]

University of Rochester, Rochester, NY 14627, USA

O.D. FACKLER and K.A. JENKINS [7]

Rockefeller University, New York, NY 10021, USA

Received 16 November 1984

We describe a high statistics measurement from deep inelastic neutrino–nucleon scattering of the electroweak parameters ρ and $\sin^2\theta_W$, performed in the Fermilab narrow-band neutrino beam. Our measurement uses a radius-dependent cut in $y = E_H/E_\nu$ which reduces the systematic error in $\sin^2\theta_W$, and incorporates electromagnetic and electroweak radiative corrections. In a renormalization scheme where $\sin^2\theta_W \equiv 1 - m_W^2/m_Z^2$, a value of $\sin^2\theta_W = 0.242 \pm 0.011 \pm 0.005$ is obtained fixing $\rho = 1$. If both $\sin^2\theta_W$ and ρ are allowed to vary in a fit to our data, we measure $\rho = 0.991 \pm 0.025 \pm 0.009$.

Introduction. We report a measurement of the electroweak parameters $\sin^2\theta_W$ and ρ from deep inelastic scattering of muon neutrinos and antineutrinos on iron nuclei using the Fermilab narrow band [1] neutrino beam. These parameters are extracted from the Paschos–Wolfenstein ratios [2]

$$R^{\pm} = \frac{d\sigma_{NC}^{\nu}/dy \pm d\sigma_{NC}^{\bar{\nu}}/dy}{d\sigma_{CC}^{\nu}/dy \pm d\sigma_{CC}^{\bar{\nu}}/dy}, \qquad (1)$$

where $y \equiv$ hadron energy (E_H)/incident neutrino energy (E_ν). For an isoscalar target with no strange quark sea, these ratios have the simple theoretical

[1] Present address: University of Toronto, Toronto, Ontario Canada, M5S1A7.
[2] Present address: SLAC, Stanford, CA 94305, USA.
[3] Present address: Hughes Aircraft Co., El Segundo, CA 90245, USA.
[4] Present address: Fermilab, PO Box 500, Batavia, IL 60510, USA.
[5] Present address: National Laboratory for High Energy Physics, Tsukuba-gun, Ibaraki-ken 305, Japan.
[6] Present address: Institute for High Energy Physics, Beijing, People's Republic of China.
[7] Present address: IBM Thomas J. Watson Research Center, PO Box 218, Yorktown Heights, NY 10598, USA.

form (neglecting higher order radiative corrections)

$$R^- = \rho^2(\tfrac{1}{2} - \sin^2\theta_W) \,, \qquad (2a)$$

$$R^+ = \rho^2(\tfrac{1}{2} - \sin^2\theta_W + \tfrac{10}{9}\sin^4\theta_W) \,, \qquad (2b)$$

independent of y. Both R^- and R^+ are used to give the best statistical precision. This is mathematically equivalent to using both $R^\nu = \sigma^\nu_{NC}/\sigma^\nu_{CC}$ and $R^{\bar\nu} = \sigma^{\bar\nu}_{NC}/\sigma^{\bar\nu}_{CC}$.

A novel feature of this analysis is the imposition of a radius-dependent cut in the kinematic variable y which reduces the systematic and total error.

Beam and apparatus. The neutrino beam was produced by steering 400 GeV/c protons onto a primary target, creating secondary pions, kaons and protons. After momentum and sign selection, the secondary beam had an RMS momentum spread of 9% and an RMS angular divergence of 0.15 mrad. The secondary beam was directed down a 340 m long pipe where pions and kaons decayed to produce muon neutrinos or antineutrinos, accompanied by muons. The surviving secondaries were absorbed in a beam dump, which was followed by a steel and earth muon shield.

The position, intensity and composition of the secondary beam were measured to allow calculation of the neutrino flux at the detector. Neutrinos from pion and kaon decay formed two distinct energy bands; for each band, the transverse position of the interaction in the detector and the energy of the incident neutrino were correlated.

Five settings of the secondary beam momentum were used for both neutrinos and antineutrinos: 120, 140, 168, 200, 250 GeV/c. Data were taken from June 1979 to January 1980.

The detector has been described elsewhere in detail [3,4]. It comprises a hadron calorimeter made of 690 tons of steel plates, instrumented with spark chambers (every 20 cm of steel) and 305 cm × 305 cm liquid scintillation counters (every 10 cm of steel), followed by an instrumented steel toroidal muon spectrometer. The RMS hadron shower energy resolution, measured directly in hadron test beams, was found to be well fitted by the expression [5,6]

$$\delta E_H = (0.72 \pm 0.20) + (0.81 \pm 0.03)\sqrt{E_H} \,.$$

Data analysis. The event trigger used for this analysis required an energy deposition of more than 12 GeV in the calorimeter. To avoid bias between neutral current (NC) and charged current (CC) events, the fitted track and spectrometer-analyzed momentum of the CC final state muon were not used: the analysis relied primarily on calorimetric information. The event length, defined as the longitudinal distance over which energy was deposited in the calorimeter, was used to separate NC and CC events. For NC events the length is the range of the hadron shower, whereas for CC events it is typically determined by the range of the muon. The transverse vertex of the event, used for fiducial cuts and in the calculation of the incident neutrino energy E_ν, was determined from a weighted average of spark coordinates in the hadron shower. The RMS transverse vertex resolution in either the vertical or horizontal directions was found to be 4.3 cm, independent of secondary beam momentum.

Longitudinal and radial fiducial cuts (radius less than 102 cm) were imposed which ensured that the hadron shower was fully contained. In addition, a software hadron energy cut of 20 GeV was imposed to ensure that the NC trigger was 100% efficient. The efficiency of the NC trigger was measured as a function of E_H with an independent trigger.

Since the maximum energy of a neutrino from pion decay (ν_π) is 43% of the secondary beam energy, whereas the maximum energy of a neutrino from kaon decay (ν_K) is 95% of the secondary beam energy, the ratios $R^\pm$ were formed separately for the ν_π and ν_K classes.

In a separate analysis of the CC data [4,7], the measured E_ν (measured hadron energy + measured muon momentum) of CC events was plotted versus event radius, R, for each beam setting. From these plots, the dichromatic nature of the beam was clearly evident, since the data lay in two distinct bands corresponding to ν_π and ν_K events. For each beam setting, a curve $E_{sep}(R)$ was drawn which separated the two bands.

Since only E_H (and not E_ν) could be measured for NC events, the measured E_H was used to separate ν_π and ν_K events in this analysis. We defined the ν_K class to consist of events with $E_H > E_{sep}(R)$, and the ν_π class to consist of events with 20 GeV $\lesssim E_H < E_{sep}(R)$. The ν_K class had no ν_π contamination. However, the ν_π class contained a background of ν_K events with low hadron energy which was subtracted by a Monte Carlo calculation.

From a study of hadron showers in neutrino interactions and in hadron beam calibration data at different energy settings [5], it was found that <0.7% of hadron showers in our detector penetrated beyond 210 cm of steel. Events with lengths ⩽210 cm of steel were defined to be in the "NC" class; events with lengths >210 cm of steel were defined to be in the "CC" class, and had the contribution from muon ionization subtracted from the measured E_H.

The "NC" class defined above contained short length CC events, where the final state muon either ranged out or left the target at a wide angle, θ_μ. In both cases, the event would have to be at large y, since $E_\mu = E_\nu(1-y)$ and $E_\nu\theta_\mu^2 \sim 2m_N xy/(1-y)$, where m_N is the nucleon mass. A Monte Carlo calculation indicated that 21.7% of events in the "NC" class were actually CC events.

To reduce this large CC background, a novel radius dependent cut on the kinematic variable $y = E_H/E_\nu$ was imposed to eliminate the ambiguous large y region. This cut was derived by requiring the final state lepton to penetrate further than 210 cm Fe, corresponding to a spatial distance L_{cut} = 427 cm in the calorimeter, so that if it were a muon, it would be identified as such. This translated into requiring that at a radius R, an event must have had

$$y < y_{cut}(R) \equiv \frac{E_\nu[\tan^{-1}((152\ \mathrm{cm} - R)/L_{cut})]^2}{2M_N + E_\nu[\tan^{-1}((152\ \mathrm{cm} - R)/L_{cut})]^2} .$$

This cut was applied assuming the interacting neutrino was ν_K or ν_π as appropriate, with E_ν determined from the radius R and the secondary beam energy. Note that R^+ and R^- are independent of y and are therefore not affected by this cut.

If the secondary beam had zero angular and momentum dispersion, this cut would ensure there would be no CC events in the "NC" class. Due to the finite beam dispersion, and the finite E_H resolution there was still a small CC contamination (4.6%) of the "NC" class after the radius dependent y cut had been imposed. Application of the radius dependent y cut reduced the event sample by 54% ond reduced the CC contamination of the "NC" class by a factor of five. The effect of this cut is illustrated in fig. 1.

The small cosmic ray background was subtracted using events taken during an off-beam-spill gate. The wide band background was subtracted using events taken with the momentum selection collimator closed. In addition, corrections were made for the inefficieny in finding a good transverse vertex, and for NC events with length greater than 210 cm Fe. The net effect of all the corrections discussed in this paragraph was typically ~1% for neutrino data and typiallcy ~4% for antineutrino data (except for the $\bar{\nu}_K$ "NC" class, which had a wide band background of 16%).

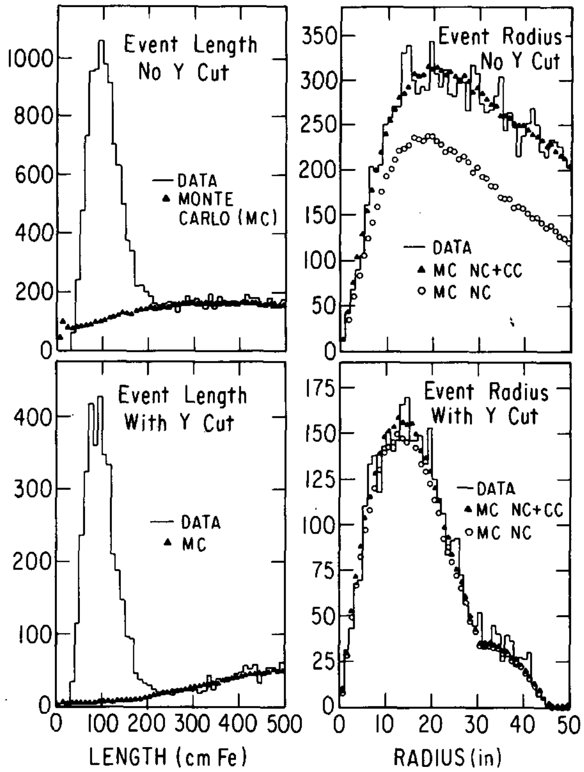

Fig. 1. Effect of radius-dependent y cut (E_H > 20 GeV, total ν sample). The event radius plots contain events with lengths less than L_{cut}; the difference between the Monte Carlo NC + CC and NC points is due to short length CC events.

The dependence on Monte Carlo simulation was reduced by using the radius dependent y cut. However, Monte Carlo corrections had to be made to the data sample for (1) ν_K events with low E_H in the ν_π sample; (2) ν_e charged and neutral currents events (from Ke3 decays) which mimic NC events; (3) the small background of CC events remaining in the "NC" sample.

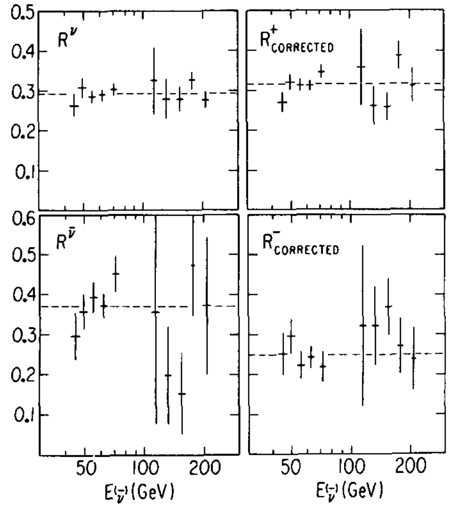

Fig. 2. $R^{\nu}, R^{\bar{\nu}}, R^{+}_{\text{corrected}}, R^{-}_{\text{corrected}}$ versus mean (anti-) neutrino energy. The dashed lines are the average values.

The Monte Carlo used structure function parametrizations obtained in a fit to our CC data [5,6,8]. The Monte Carlo contained slow rescaling ($M_{\text{charm}} = 1.5$ GeV/c^2), a strange sea taken to be half SU(3) symmetric ($s/\bar{u} = 0.5$), electromagnetic radiative corrections [9] (from virtual photon diagrams and bremsstrahlung by the CC final state muon), and QCD evolution of the structure functions.

Monte Carlo events were analyzed in exactly the same way as the data. In order to avoid dependence on flux monitoring, they were normalized directly to data events (separately for ν_π and ν_K, taking into account the ν_K background [10] in the ν_π class). The Monte Carlo simulation showed that the combined ν_π and $\bar{\nu}_\pi$ classes contained an 8.2% background [10] of ν_K or $\bar{\nu}_K$ events with low hadron energy. The background from ν_e events [10] was 0.6% for the combined ν_π and $\bar{\nu}_\pi$ "NC" classes and amounted to 22% for the combined ν_K and $\bar{\nu}_K$ "NC" classes.

After the corrections described above have been applied, the ratios $R^{\nu,\bar{\nu}}, R^{\pm}$ can be formed. $R^{\pm}$ incorporates (anti-) neutrino fluxes derived from our secondary flux measreuments. R^{ν} and $R^{\bar{\nu}}$ are plotted versus mean ν_π or ν_K energy for the different beam settings, in fig. 2.

Extraction of $\sin^2\theta_w$ *and* ρ. The measured $R^{\pm}$ values, $R^{\pm}_{\text{meas}}$, were corrected for the non-isoscalar target, the finite strange quark sea, charm production, electromagnetic radiative corrections, and slight differences in the $\nu, \bar{\nu}$ energy spectra before using eqs. (2a), (2b). For each beam setting, values $R^{\pm}_{\text{SIM}}$ were obtained by simulating our measurement, including the above effects. Electromagnetic radiative corrections within our y cuts, from virtual photon diagrams and bremsstrahlung by the final state CC muon, were included in the simulation using the method described in ref. [9]. The simulation used an input value $\sin^2\theta_{\text{W}_0}$, which was substituted into eqs. (2a), (2b) to give $R^{\pm}_0$. The correction factors $f^{\pm}$ for each beam setting were defined to be $R^{\pm}_0/R^{\pm}_{\text{SIM}}$, and in general $|1 - f^{\pm}| < 3\%$. The inclusion of various effects in calculation of $f^{\pm}$ resulted in the variations in $\sin^2\theta_{\text{w}}$ shown in table 1.

Table 1
Variations in $\sin^2\theta_{\text{W}}$.

	$\delta \sin^2\theta_{\text{W}}$
non-isoscalar target	–0.009
non-strange sea	+0.002
strange quarks + slow rescaling ($s/\bar{u} = 0.5, m_c = 1.5$ GeV/c^2)	+0.004
electromagnetic radiative corrections	–0.002
$\nu, \bar{\nu}$ flux spectral differences	+0.0002

Additional electroweak radiative corrections must be made which depend on the renormalization scheme used. We have chosen the convention [11,12] [‡1] in which $\sin^2\theta_{\text{w}}$ is defined by $\sin^2\theta_{\text{w}} \equiv 1 - m^2_{\text{W}}/m^2_{\text{Z}}$, where m_{W} and m_{Z} are the physical gauge boson masses. Using this convention, we incorporated the electroweak radiative correction due to the higher order CC Wγ box diagram in a separate correction factor [11, 13] $f_{\text{W}\gamma} = 0.983$. This factor was calculated with no y cuts; the small uncertainty in the effect of our y cuts on $f_{\text{W}\gamma}$ is included in our systematic error [13,14]. (Two further radiative corrections to $\sin^2\theta_{\text{w}}$ were not included because they almost exactly cancel: –0.0007 from terms containing logarithms of quark masses [11], and +0.0007 from vertex diagrams involving photons and γZ mixing diagrams [12].)

We then extracted $\sin^2\theta_{\text{w}}$ and ρ from

$$R^{-}_{i\,\text{corrected}} = f^{-}_i R^{-}_{i\,\text{meas}} = f_{\text{W}\gamma}\,\rho^2(\tfrac{1}{2} - \sin^2\theta_{\text{w}})\,, \quad \text{(3a)}$$

‡1 The correction of +0.0007 [12] corresponds to $1/\kappa^{(\nu_\mu;h)}$ (–20 GeV^2) = 1/0.997. See also eq. (16c) of ref. [11].

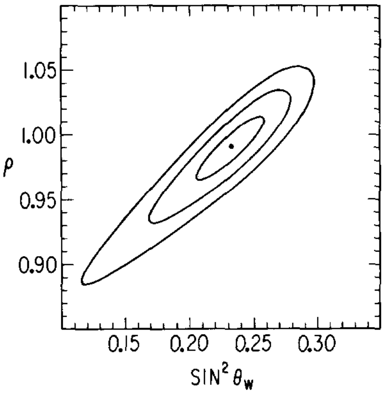

Fig. 3. ρ versus $\sin^2\theta_W$. 1σ, 2σ, 3σ contours are shown for the two-parameter fit.

$$R^+_{i\,\mathrm{corrected}} = f^+_i R^+_{i\,\mathrm{meas}} = f_{W\gamma}\rho^2(\tfrac{1}{2} - \sin^2\theta_W + \tfrac{10}{9}\sin^4\theta_W)\,, \quad (3b)$$

where i runs over the ν_K and ν_π classes for the 5 secondary beam settings. The values of $R^\pm_{\mathrm{corrected}}$ are plotted in fig. 2. The mean $R^+_{\mathrm{corrected}}$ was 0.317 ± 0.007 and the mean $R^-_{\mathrm{corrected}}$ was 0.249 ± 0.015.

Results. A one-parameter fit to our data, with ρ fixed at 1, gives

$$\sin^2\theta_W = 0.242 \pm 0.011 \pm 0.005\,. \quad (4a)$$

in the renormalization scheme where $\sin^2\theta_W \equiv 1 - m^2_W/m^2_Z$. The errors are statistical and systematic, respectively.

A two-parameter fit gives

$$\rho = 0.991 \pm 0.025 \pm 0.009\,, \quad (4b)$$

$$\sin^2\theta_W = 0.234 \pm 0.026 \pm 0.010\,.$$

Eqs. (4a), (4b) are our best determination of the electroweak parameters. The 1, 2, and 3 standard deviation contours for the two-parameter fit are shown in fig. 3. The errors in fig. 3 are statistical only.

If we express our result as the angle $\sin^2\hat{\theta}_W(m_W)$ defined in the $\overline{\mathrm{MS}}$ renormalization scheme commonly used in GUTS, the value in eq. (4a) would be reduced by a factor [15,16] of 1.006, to give

$$\sin^2\hat{\theta}_W(m_W) = 0.240 \pm 0.011 \pm 0.005\,.$$

Had we ignored electroweak corrections altogether (corresponding to $f_{W\gamma} = 1$ in eq. (3)) our value of $\sin^2\theta_W$ for the one-parameter fit would have been increased by +0.008.

An innovative fateure of this analysis was the use of a radius-dependent y cut. To illustrate the effect of this cut on both the value and error for $\sin^2\theta_W$, an identical analysis was performed (including subtraction of the ν_K background from the ν_π class) except that the radius-dependent y cut was not imposed. In this case, a one-parameter fit (with $\rho = 1$) gives

$$\sin^2\theta_W = 0.237 \pm 0.009 \pm 0.012\,,$$

and a two-parameter fit gives

$$\rho = 0.994 \pm 0.018 \pm 0.011\,,$$

Table 2
Systematic errors in $\sin^2\theta_W$.

	With radius-dependent y cuts	No radius-dependent y cuts
flux uncertainty (e.g. in π/K fractions)	±0.001	±0.001
Monte Carlo subtractions (includes an estimated uncertainty of ±8% in the CC subtraction)	±0.002	±0.011
$R^\pm$ correction factors $f^\pm$ (overall level of $q\bar{q}$ sea (±10%) $s/\bar{u}$ = 0.5 ± 0.2)	±0.0003	±0.0005
$\cos\theta_{\mathrm{Cabibbo}}$ = 0.9737 ± 0.0025	±0.0003	±0.0002
M_c = 1.5 ± 0.2 GeV	±0.003	±0.002
uncertainties in radiative corrections	±0.002	±0.002
hadron energy (systematic uncertainty in E_H < ±2%)	±0.002	±0.002
mean π, K momentum (uncertain to ±1.5%)	±0.001	±0.001
momentum bite: (σ_p/p = 9% ± 1%)	±0.002	±0.001
variations in fitting procedures	±0.001	±0.002
total systematic error	$\delta \sin^2\theta_W$ = ±0.005	$\delta \sin^2\theta_W$ = ±0.012

$\sin^2\theta_W = 0.227 \pm 0.018 \pm 0.017$.

Although the statistical error is smaller without the radius dependent y cut, systematic errors are increased by over a factor of 2 due to the larger CC background in the NC sample (21.7% without y cuts, 4.6% with y cuts). The sources of systematic error with and without this cut are listed in table 2.

Conclusions. The radius dependent y cut used in this experiment has reduced the relative CC background by a factor of five, and has consequently reduced the systematic error in $\sin^2\theta_W$. This is an important advangage since the calculation of CC background otherwise requires an extrapolation into the poorly measured high y region. The systematic error without this cut is dominated by the uncertainty in the CC contamination of the "NC" class (table 2). The systematic error in this contamination, due primarily to uncertainties in the quark x-distributions, is the most uncertain of our systematic errors; we conservatively estimate that the CC contamination has a fractional error of ±8%. At present, the use of the radius-dependent y cut results in a smaller total error, and therefore gives our best measurement of $\sin^2\theta_W$ and ρ. However, with more precise determination of structure functions in the future, this may no longer be the case.

Our value of $\sin^2\theta_W = 0.242 \pm 0.011 \pm 0.005$ can be compared directly to the results of the CERN collider experiments [17] [‡2]. Our value is slightly larger, but is consistent with, the values obtained from the measured W masses alone (although lower than the value obtained by UA1 using both their measured W and Z masses). It is also consistent with the value obtained from other neutrino experiments [18] [‡3].

‡2 From the relationship $\sin^2\theta_W = 1 - m_W^2/m_Z^2$, UA1 and UA2 obtain $\sin^2\theta_W = 0.284 \pm 0.035$ and 0.196 ± 0.040 respectively, directly from their measured masses. The collider experiments can make a more precise determination using the relation [16] $\sin^2\theta_W = (38.65\ \mathrm{GeV}/m_W)^2$, which incorporates radiative corrections. UA1 and UA2 then obtain $\sin^2\theta_W = 0.228 \pm 0.008 \pm 0.014$ and $\sin^2\theta_W = 0.216 \pm 0.010 \pm 0.007$ respectively. (The result quoted in Arnison et al. is 0.002 lower, and corresponds to $\sin^2\hat{\theta}_W(m_W) = [38.65\ \mathrm{GeV}/(\sqrt{1.006}\,m_W)]^2$, in the $\overline{\mathrm{MS}}$ renormalization scheme.)

‡3 Ref. [18] extracts $\sin^2\hat{\theta}_W(m_W) = 0.226 \pm 0.012$ and $\sin^2\hat{\theta}_W(m_W) = 0.280 \pm 0.016$ from CDHS (1984) and CHARM (1981) data, respectively. This is to be compared to our result of $\sin^2\hat{\theta}_W(m_W) = 0.240 \pm 0.011 \pm 0.005$.

In the $\overline{\mathrm{MS}}$ renormalization scheme, our value of $\sin^2\hat{\theta}_W(m_W) = 0.240 \pm 0.011 \pm 0.005$ can be compared to the prediction of the minimal SU(5) model [19] that $\sin^2\hat{\theta}_W(m_W) = 0.214^{+0.004}_{-0.003}$. Minimal supersymmetric GUTS with two light Higgs supermultiplets predict [19] $\sin^2\hat{\theta}_W(m_W) = 0.236 \pm 0.003$. Clearly our value does not support minimal SU(5) but is consistent with supersymmetry.

Our value of $\rho = 0.991 \pm 0.025 \pm 0.009$ is in good agreement with the expectation of the standard model that $\rho = 1$. It can be compared with the values obtainde by UA1 and UA2 of $\rho = 0.928 \pm 0.05$ and $\rho = 1.02 \pm 0.06$ respectively [17].

References

[1] D.A. Edwards and F.J. Sciulli, A second generation narrow band beam, Fermilab TM-660, unpublished.
[2] E.A. Paschos and L. Wolfenstein, Phys. Rev. D7 (1973) 91;
P.Q. Hung and J.J. Sakurai, Phys. Lett. 63B (1976) 295.
[3] B.C. Barish et al., IEEE Trans. Nucl. Sci. 25 (1978) 532.
[4] R. Blair, Ph.D. thesis, California Institute of Technology (1982), unpublished;
R. Blair,et al., Monitoring and calibration system for neutrino flux measurement in a high energy dichromatic beam, Fermilab Pub. 83/26-EXP, Nucl. Instrum. Methods, to be published.
[5] D.B. MacFarlane, Ph.D. thesis, California Institute of Technology (1984), unpublished (available as Nevis preprint R#1297).
[6] M.V. Purohit, Ph.D. thesis, California Institute of Technology (1984), unpublished (available as Nevis preprint R#1298).
[7] R. Blair et al., Phys. Rev. Lett. 51 (1983) 343.
[8] D.B. MacFarlane et al., Nuclear structure functions from high energy interactions with iron and QCD results, Z. Phys. C, to be published.
[9] A. de Rújula, R. Petronzio and A. Savoy-Navarro, Nucl. Phys. B154 (1979) 394.
[10] P.G. Reutens et al., preprint EFI 84-23, to be published in: Proc. 11th Intern. Conf. on Neutrino physics and astrophysics (Dortmund, 1984).
[11] A. Sirlin and W.J. Marciano, Nucl. Phys. B189 (1981) 442.
[12] W.J. Marciano and A. Sirlin, Phys. Rev. D22 (1980) 2695, eq. (25d).
[13] E.A. Paschos, private communication.
[14] A. de Rújula, private communicaton.
[15] S. Sarantakos, A. Sirlin and W.J. Marciano, Nucl. Phys. B217 (1983) 84.
[16] W.J. Marciano and A. Sirlin, Phys. Rev. D29 (1984) 5;

W.J. Marciano, preprint BNL-34728, to be published in: Proc. 4th Topical Workshop on Proton antiproton collider physics (Bern, 1984).

[17] UA1 Collab., G. Arnison et al., Phys. Lett. 129B (1983) 273;
UA2 Collab., P. Bagnaia et al., Z. Phys. C 24 (1984) 1;
P. Langacker, preprint UPR-0270T, to be published in: Proc. 22nd Intern. Conf. on High energy physics (Leipzig, 1984).

[18] C. Geweniger, to be published in: Proc. 11th Intern. Conf. on Neutrino physics and astrophysics (Dortmund, 1984).

[19] J. Ellis, Proc. Intern. Symp. on Lepton and photon interactions at high energies (Cornell, 1983);
J. Ellis, D.V. Nanopoulos and S. Rudaz, Nucl. Phys. B202 (1982) 43;
M.B. Einhorn and D.R.T. Jones, Nucl. Phys. B196 (1982) 475.